Recent Advances in X-ray Cone-beam Computed Laminography

Neil S. O'Brien*[1], Richard P. Boardman†[1], Ian Sinclair‡[1] and Thomas Blumensath§[1,2]

[1]μ-VIS X-ray Imaging Centre, University of Southampton, UK

[2]Institute for Sound and Vibration Research, University of Southampton, UK

May 23, 2016

Abstract

X-ray computed tomography is a well established volume imaging technique used routinely in medical diagnosis, industrial non-destructive testing, and a wide range of scientific fields. Traditionally, computed tomography uses scanning geometries with a single axis of rotation together with reconstruction algorithms specifically designed for this setup. Recently

*corresponding author; email nsob1c12@soton.ac.uk, tel: +44(0)2380593468, fax: +44(0)2380593016

†rpb@soton.ac.uk

‡is1@soton.ac.uk

§Thomas.Blumensath@soton.ac.uk

there has however been increasing interest in more complex scanning geometries. These include so called X-ray computed laminography systems capable of imaging specimens with large lateral dimensions, or large aspect ratios, neither of which are well suited to conventional CT scanning procedures. Developments throughout this field have thus been rapid, including the introduction of novel system trajectories, the application and refinement of various reconstruction methods, and the use of recently developed computational hardware and software techniques to accelerate reconstruction times. Here we examine the advances made in the last several years and consider their impact on the state of the art.

Keywords: Cone-beam, computed laminography, reconstruction algorithms, X-ray tomography, X-ray laminography, tomosynthesis.

1 Introduction

Since the early days of computed tomography (CT), there have been advances across all aspects of the technique, both in image acquisition and reconstruction. Early CT scanners made use of a single-crystal NaI detector coupled with a photomultiplier. Scanning a single plane in a three dimensional volume would take several minutes. A typical sample volume of $3\,\mathrm{mm}^2 \times 13\,\mathrm{mm}$ could be reconstructed using an algebraic reconstruction technique (ART) into slices, each of 80×80 pixels and taking around 7 minutes [10]. The advent of the filtered backprojection (FBP) reconstruction method reduced the time per slice to 30 seconds and increased the slice resolution to 160×160 pixels. Today's CT scanning systems can yield scans consisting of tens of gigabytes of image data in the form of several thousand projections, each up to 4096×4096 (using e.g. the PerkinElmer XRD 1611 xP detector [65]) or more pixels. Cone beam projection data can be reconstructed using the Feldkamp-Davis-Kress (FDK) filtered backprojection algorithm, implemented in commercially available software on mass-produced graphics processing units (GPUs), taking just several minutes to reconstruct the entire volume.

The CT scanning and reconstruction process, however, remains best suited to approximately cylindrical objects, i.e. those with an aspect ratio of approximately unity in the plane normal to the axis of rotation. When the path lengths through the scanned object vary dramatically at different angles, or where the physical extents of the sample being scanned preclude a full rotation within the scanner, then conventional CT scanning techniques may only produce incomplete data as, for example, X-rays may be absorbed completely along the longest path. These conditions produce increasingly poor reconstruction re-

sults as the aspect ratio of the sample increases. Several techniques may yield improved imaging quality in such cases, and the choice of technique will be dependent upon many factors. It is sometimes possible to improve the aspect ratio of the samples, either by stacking multiple samples together or by physically cutting tokens from the sample, if destructive testing is permissible. Alternatively, dual-energy CT scanning has been developed and applied to the imaging of CFRP panels [68]: radiographs are acquired using two accelerating voltages, the higher being optimised for the long path-lengths in the sample and the lower being optimised for the shorter path lengths. The two sets of radiographs are combined prior to reconstruction; the dual-energy technique was found to improve both the contrast-to-noise and signal-to-noise ratios of the reconstructed images.

Another approach, that which we focus on in the present paper, is laminographic scanning and reconstruction. In laminographic scanning, it is advantageous to vary the motion of the sample as well as the method of reconstructing the scanned data from conventional CT. Classical laminography was perhaps first proposed by the dermatologist André Bocage in 1916, using an X-ray film and tube moving linearly in opposite directions, to record a crisp image of a single fixed plane in the sample, since each point in the chosen plane would cast its image in the same place on the film [45]. More recent work has demonstrated that computed laminography (CL), where a high resolution flat panel detector is moved along a suitable trajectory, and a reconstruction technique modified from CT is used to resolve many layers of the sample in detail, can produce better-quality images than a limited-angle CT scan, especially where the limitation on angular range is severe [82]. The effectiveness of CL has

been demonstrated recently in the assessment of impact damage to carbon-fibre composites, where synchrotron-radiation CL was used to deliver a short scan time and high image quality [13].

In this article, we will review existing methods for computed laminography, specifically detailing the trajectories and reconstruction methods involved. CL has been used at synchrotron beamlines where a parallel beam is available, allowing objects sized up to several dm across to be scanned with considerably better resolution of fine details than limited-angle CT [40]. We shall however largely restrict ourselves in this article to the cone-beam case, as produced by many compact laboratory sources. A review of synchrotron-radiation CL was recently produced by other researchers [41].

We will adopt a working definition of laminography as a 3-D imaging process of acquiring X-ray projections and performing a reconstruction, where the amount of data collected is less than that required for a full CT scan, due – for example – to access constraints imposed by the geometries of the sample and the imaging system. The current article is structured as follows: we firstly explore the trajectories and geometries that have been applied in CL systems in § 2. We then detail the various reconstruction methods that have been used in laminography in § 3; because most advanced laminographic reconstruction methods have their roots in CT, we include significant literature on the various methods as applied to CT as well as to laminographic reconstructions. In § 3.5 we consider recent developments in computational technologies that facilitate accelerated implementations of these reconstruction methods. Finally we give a summary and outlook in § 4.

2 Trajectories and geometries for cone-beam laminography

Various system motions have been discussed in the literature, each having their advantages and disadvantages. The following subsections offer more detail on some of the possible system motions that have been used in laminography systems.

The system geometry and trajectory which define the relative motions between X-ray source, detector and object are crucial aspect of the design of a CL system, as they can place a limit on the total amount of information that may be recorded and therefore used in any reconstruction. To ensure that all volumetric information is captured by a cone-beam CT system, a set of sufficiency criteria has been derived [79]. These require that the curve followed by the source (which sits at the vertex of the cone-beam) remains outside the region of the object, is bounded, continuous and differentiable almost everywhere and that every plane passing through the region of interest must cut the trajectory at least once. This means that many systems can only produce approximate reconstructions. Laminographic trajectories preclude capturing data from a range of angles which would be captured during full CT, so that laminographic scans contain less information than CT scans. In practice, it is thus important to tune the trajectory geometry of a laminographic system to balance the trade-off between the amount of data captured against other parameters such as the dimensions of specimens that may be imaged and the relative angles of components. An example of such an optimisation for a circular laminographic trajectory is given by [66].

Other physical considerations influence the choice of a scan trajectory in practice. It is conceptually of little importance if we move the object or the source and detector. For example, in traditional X-ray CT, the data collected if we fix the object and rotate source and detector is equivalent to the data generated with a fixed source and detector whilst rotating the object. However, there are obvious practical differences between the two approaches. The same is true in laminography. It is the relative motion between source, object and detector that provides the diversity in information required for three dimensional image reconstruction. Yet practical constraints limit potential movement trajectories, and accuracy requirements might make it more sensible to use a specific physical realisation of a relative movement trajectory. For example, translating the sample works well for small and lightweight objects, such as circuit boards, but may become problematic if larger, bulkier samples have to be moved accurately over larger distances [46, 57]. Other constraints related to the sample may dictate that the relative motion should arise from the motion of the sample or the X-ray source and detector. One example is that for *in vivo* measurement such as e.g. in medical scanning of human patients, or in imaging of a mouse's physiological functions, it is preferable to position the animal horizontally and rotate the imaging system around it [16, 19]. On the other hand, in nondestructive testing CT applications, it is more typical to place the object on a rotation stage and keep the imaging system still [19]. Yet more complex trajectories are also possible. Extreme examples would be the computed laminography machine reported in [53], where source, detector and object are all moved, or the option put forward in [12] where multiple detectors and a multiple-anode scanning electron beam X-ray source is used to record projections from many

angles in a short time frame. Whilst the latter approach avoids system motions completely, the former allows objects larger than the scanner's usual maximum dimensions to be accommodated.

We classify typical scan geometries into the following four categories: planar, swing, rotary, and more complex geometries that do not neatly fall into the three other categories. Schematic diagrams that exemplify motions belonging to each of the categories are given in Figures 4, 4, 4, and 4 respectively.

2.1 Planar

In a planar system, the source, detector and object to be scanned each remain in their own plane and a relative motion is set up between them. An X-ray source with a suitably wide cone-beam angle is usually required to illuminate the detector in all its positions during the translation. Two common planar motions are those using linear and circular paths.

Probably the simplest planar motion is as illustrated schematically in Fig. 4, in which the source and detector are translated along straight lines parallel to the plane of the sample. This is detailed in the 'Linear' subsection, below. A similar movement pattern, in which source and detector move in circular paths, is shown in figure 4. Again, this motion can be designed so that points on one focal plane are mapped to the same points on the detector. This will lead to a simplified tomosynthesis reconstruction as discussed below, but more general planar motions are also possible in conjunction with somewhat more involved reconstruction techniques.

2.1.1 Linear

If the object remains stationary, the source and detector may be translated linearly through space. Such a linear path is shown schematically in Fig. 4, where the source and detector move in opposite directions in such a manner that each point in a focal plain in the object is mapped to the same detector location. Knowing the relative positions of each component (source, detector, sample) for each frame, the resulting image may be reconstructed to a volume. Alternatively, keeping both the source and detector stationary, good results have been achieved by translating just the object along a linear path within the cone-beam of the source [85].

This cone-beam CL approach is equivalent to the CT approach with a limited aperture [31, 85], so that slightly-modified CT reconstruction algorithms may be taken advantage of to reconstruct the data. A similar setup was proposed in 2007 by Gao et al. who described a "linear CT" (LCT) system for security and industrial applications with fixed source and detector, where the sample is translated along a line, equivalent to keeping the sample still and translating the source and detector [28].

Linear motion may lead to different resolutions in the x and y axes of the sample, which is not always desirable [53]. The linear motion gives short acquisition times [27], but acquires relatively little information, making clear reconstructions challenging.

2.1.2 Circular

The object and detector may be translated in circles within their planes. This is a more complicated motion but gives the advantage of equality of the resolu-

tions in the x and y directions in the sample [53]. In this setup, the detector and source are moved around a common centre, remaining in their parallel planes, with a phase difference of π, as illustrated in Fig. 4. The line from the centre of the source aperture to the centre of the detector at any time during the scan should pass through the same point in the middle layer of the sample plane during the entire rotation.

The design parameters of circular trajectories are addressed specifically by [66] for the case of laminography for planar samples using tomosynthesis reconstruction as discussed below, with some brief additional consideration of other reconstruction techniques. The authors recommend using a configuration where there are many different tilt angles, to reduce the occurrence of hat-shaped artefacts and maintain good contrast and sharpness.

2.2 Swing or limited-angle tomography

Also known as limited angle tomography, a swing laminographic scan [57, §4.2] may be completed in a standard CT scanner using a limited angular range of e.g. $\pm 30^\circ$ rather than the full $\pm 180^\circ$ required for cone-beam CT, as illustrated in Fig. 4. This scanning geometry can be used in combination with different reconstruction techniques. Its relationship to standard tomography means that many standard CT algorithms can be adapted; it is also a ubiquitous technique in electron tomography, discussed in, for example [20, 22].

2.3 Rotary

In this technique, the planar object is rotated along an axis normal to its surface, which is inclined with respect to the principal ray of the X-ray beam [57, §4.3],

as illustrated in Fig. 4. The motion is equivalent to cone-beam CT where the specimen is mounted some distance above (or below) the principal axis. Both the source and detector are kept in fixed positions, the beam passing through the specimen at an angle to the axis of rotation. The motion is simplified as there is only one moving part, which simply rotates; the source-detector position remaining constant means that the geometry should not introduce any variations in detected intensity throughout the trajectory, so fewer detector calibrations are necessary. In one scheme, the detector is mounted on an arc-shaped guide rail, and the specimen is rotated on a stage in the illumination of the cone-beam [84]. The motion of the detector along its arc allows for changing the laminographic angle (i.e., the angle between the axis of rotation and the normal to the principal ray).

For the rotary trajectory, in the parallel beam case it is possible to map individual sampling planes into Fourier space straightforwardly, yielding a representation of the sampled regions and those in which no information is available. This is illustrated by *e.g.* Helfen et al in [39, Figure 2], and Xu *et al* in [82, Figure 1]. In the cone-beam case, the correspondence between the real-space and Fourier domains is considerably more complicated, but where cone-beam projections may be re-binned to equivalent parallel-beam projections, these mappings may apply approximately, and provide additional insight into the information available from a given scan.

The rotary geometry has also been successfully applied in phase-contrast computed laminography (PC-CL), which is ideal for imaging specimens of weak absorption contrast. In PC-CL, conventional CL is expanded upon to extract phase information, and this has been reported on for both the cone-

beam and parallel-beam cases [2, 26]. The method introduced by Fu et al. [26] is designed to be used with cone-beam laboratory sources, and uses a modified backprojection algorithm (see below) for its reconstruction.

One recent variation of the rotary CL geometry uses a detector that is offset from the conventional central position [27]. The potential advantage of this is that the spatial resolution of conventional CL is maintained whilst an extended spatial region can be imaged for a given detector size. Numerical studies and real-world experiments yielded promising results, showing an enlarged imaging region with an improved spatial resolution.

2.4 More complex geometries and trajectories

More complex scanning geometries are also possible, especially when used with the iterative reconstruction methods discussed below. A recent example is the spherical sinusoidal scan, a scanning motion as illustrated in Fig. 4, which, used as a sparse scanning scheme, in combination with a compressed sensing-based total-variation regularised reconstruction algorithm, requires low numbers of projections to achieve good reconstructions using a numerical test phantom [1]. The new scheme is found to outperform the others in terms of resolution and contrast. The authors apply the same reconstruction methods to simulations of the other, more conventional, scanning trajectories whilst keeping the numbers of projections and detector pixels, as well as the source-to-object and source-to-detector distances, constant to show that the trajectory (and not just the reconstruction method) contributes to the enhanced quality of the results. However, to realise this sort of geometry in a real system would require complicated motion control and might only justify its use in specialist applica-

tions.

3 Reconstruction Methods

There is a close link between the scanning trajectory employed and the suitability of specific reconstruction algorithms. Whilst the simplest reconstructions simply copy analogue film based systems and thus require quite specific geometries, more advanced methods can be applied in principle to arbitrary geometries and here reconstruction performance is then often dominated by the amount of information captured in a scan. In many cases, reconstruction methods for computed laminography have been based on established techniques from the more mature field of CT, and recent advances in CT reconstruction were reviewed by Hsieh et. al. [43].

3.1 Tomosynthesis

Digital tomosynthesis (also known as focal plane tomography) mimics classical (analogue) laminography by superimposing the relevant projections. In a nutshell, digital tomosynthesis adds up all the projected images, such that all X-ray measurements that are collected along X-ray paths that pass through one point within a focal plane are mapped back to this point. This ensures that everything within the plane remains in focus in the reconstruction. Each plane parallel to the focal plane is also mapped back into the reconstructed focal plane, though it appears blurred, with the amount of blur increasing the farther away from the focal plane the parallel plane is. It therefore suffers considerable blurring, compared to contemporary CT methods, although at the

time of its introduction it produced images with a good diagnostic quality for medical purposes, using a lower dose than CT [59]. When using simple superpositions of X-ray projections to compute a digital tomosynthesis reconstruction, then the magnification must not change during the scan, which restricts geometrical configurations that may be used. The method is simple and fast but due to the relatively poor quality of the reconstruction, it is perhaps best used for simple objects which have good contrast. In digital tomosynthesis, various preprocessing steps have been suggested including methods such as taking a root to the N^{th} power, taking the mean, or applying a minimum operator iteratively to reduce the appearance of artefacts [67].

Digital Tomosynthesis can be understood as a special case of backprojection, where images are backprojected into a single focal plane. This can be done very easily for certain imaging geometries, where this backprojection leads to a simple summation of appropriately shifted projection images. More generally, when using more complex scanning geometries, then similar results can be obtained, however, individual X-ray projections might have to be preprocessed before they are combined. For example, preprocessing can correct for differences in magnification and orientation. In its most general form, this is basically a backprojection operation. In fact, if we were to sum all the backprojections of each X-ray projection throughout the volume, this would create a digital tomosynthesis type reconstruction for all potential focal planes.

3.2 Filtered Backprojection

In addition to backprojection operations, traditional CT reconstruction also routinely employs additional filtering steps within volume reconstruction, and

filtered backprojection (FBP) algorithms have long been the most popular choice among CT reconstruction methods (see, e.g. [5, 61]). These methods have a lower computational complexity than algebraic techniques whilst often reconstructing images to an acceptable quality. These algorithms were developed initially for CT reconstruction, and have more recently been adapted by various means to improve their suitability to CL reconstruction. Therefore, we will examine both the history of these methods and their recent adaptations in the following subsections.

Conventional algorithms For a parallel beam geometry, reconstruction methods begin by forming sinograms – stacks of 1D projections taken from different angles at the same sample height, arranged as a 2D image – by the Fourier slice theorem, each sinogram contains the required information to reconstruct one sample slice. The 3D reconstruction is thus turned into a series of 2D reconstructions whose results are recombined into a single volume. The standard filtered backprojection algorithm in CT reconstructs an N^3 volume from N^3 samples, having an overall algorithmic complexity of $\mathcal{O}(N^5)$. In many laminographic setups (with the exception of swing laminography with the rotation axis at 90° to the principal ray, or equivalent linear geometries), slices perpendicular to the rotation axis do not coincide with single rows of pixels on the radiographs, so the sinogram-based approach is not applicable.

Feldkamp-Davis-Kress (FDK) methods For cone-beam CT, exact FBP methods exist for certain scan geometries, though the Feldkamp-Davis-Kress (FDK) methods is the most commonly used approximation to exact reconstruction. In FDK algorithms, the recorded data are pre-weighted, compensating for the

divergent beam, then they are ramp-filtered and backprojected. The formulæ introduced by Feldkamp [25] are approximate, but their formulation is convenient for computational evaluation, gives rise to small errors in many practical situations, and is considerably faster than iterative methods such as the algebraic reconstruction techniques. Development of the FDK class of methods was motivated from considering the fan-beam reconstruction formula where the Radon transform was written as a convolution and a backprojection. The FDK method has a computational complexity of $\mathcal{O}(N^4)$. The FDK method for CT has been enhanced through the introduction of a rotation-angle-dependent weighting scheme [80] to compensate for the density drop that FDK suffers for larger cone angles. Another recent development is a further modification, to define the reconstruction slices along the exact orientation of the planar object that has been scanned [55]. This technique reduces the required reconstruction volume, and by avoiding the rotation of reconstructed images, avoids introducing additional interpolation errors into the reconstructions whilst potentially reducing the required computational time.

FBP in laminography There has been interest in adapting FBP methods for tomosynthesis for at least 15 years [54], and in that early work a general concept of filter design for laminographic reconstruction is established, and applied to one example reconstruction problem, giving rise to a "striking improvement in image quality." The main idea is to start with a simple backprojection. For several system geometries, it is then possible to evaluate the filtering effect of the forward and backward projections, an operation that effectively blurs the three dimensional volume. An inverse filter can then be

defined to undo this blurring as far as possible and this process can be optimised so that a single slice is reconstructed with high fidelity. The authors note that the spatial resolution in the plane of the reconstructed slices is good, but the depth resolution is relatively poor, which is due to the limited information available in the tomosynthetic scan. The design of filters for backprojection in tomosynthesis is also explored by [72] as well as [18]. Cho et al used a limited-angle CT arrangement, and in their reconstruction they also adapted the filter to reduce the out-of-plane artefacts, again giving rise to an anisotropic voxel size so that the reconstruction has a slice thickness which depends on the scanned angle range.

More recently FBP methods have been studied for laminographic applications such as in imaging of printed circuit boards [84], and for more general (parallel-beam) CL cases by Myagotin et al. [61]. Both of these references also use FBP type reconstruction methods. Yang et al. use a backprojection operator adapted to their laminographic scanning geometry but use the same filtering as that used in the FDK algorithm [25] used for cone-beam tomography. For the rotary laminographic setup used, this is an intuitive choice, as the scanning geometry is equivalent to a typical cone-beam CT setting, with the difference that the object is mounted well above the central slice of the cone beam. Myagotin et al. on the other hand derive their reconstruction from a backprojection filtration approach similar to that proposed in [54]. However as three dimensional filtration of the volume is deemed too costly, the 3D filter is converted to the equivalent 2D filter that can be applied before backprojection, leading again to an FBP algorithm. The 3D filter is designed for the laminographic system using the approach suggested in [60]. The work by Myagotin et al. also eval-

uates parallel and distributed computing approaches and the application of graphics processing units (GPUs) to the reduction of time required for reconstruction, and achieves a speedup for the algorithm developed of 177$\times$ for the a parallelised, distributed reconstruction running on 24 identical 8-core computers compared to sequential execution.

Using a linear laminographic system motion, Gao et al [28] considered reconstructions with two methods, both a rebinning of the data to parallel-beam projections using bilinear interpolation, and a direct linear FBP (LFBP) method that they developed without using rebinning. Their simulated results show that the rebinning-to-parallel-beam method and the LFBP produce comparable errors when there is no truncation, but that the re-binning method suffers worse errors in the presence of truncation. They further demonstrate improved reconstruction accuracy for a relatively simple simulated phantom by using the computationally-intensive IRR (iterative reconstruction reprojection) method, starting with the results of the LFBP and enforcing for each iteration the constraints of non-negativity, limitation of the scanned object region, and mass conservation of each projection in the image and projection spaces. For complex objects, though, even after tens of iterations, satisfactory reconstructions were not achieved.

Fourier methods The Fourier slice theorem provides a close link between the Fourier domain and the filtered backprojection algorithm. It is thus no surprise that many reconstruction methods work directly in the Fourier space. For example, Grangeat et al. [33] proposed an exact 3D cone-beam CT reconstruction method, in which the reconstruction is split into two parts, with an overall

complexity of $\mathcal{O}(N^4)$. The first stage is the transformation from cone-beam data to derivatives of Radon data and the second is translation from derivatives of Radon data to the 3D reconstructed object. This method offers increased robustness against distortions compared to the FDK method. Due to the similarities of the data collected by CT and CL systems, Grangeat's method may be applied to CL reconstruction for those system geometries which are equivalent to limited-view CT systems without significant modification [69]. Smith also derived a different, but structurally similar, inversion formula [76], and subsequently, this work has been integrated to provide a cone-beam reconstruction algorithm for non-planar orbits [52].

A similar method to Grangeat's was introduced by Axelsson and Danielsson in 1994, which applied direct Fourier techniques to reduce the complexity to $\mathcal{O}(N^3 \log N)$ [6]. For a complete set of projection data, their method is exact in the mathematical sense and uses the same two stages as the Grangeat method. The computational complexity of the backprojection algorithm for 3D Radon data may also be reduced to $\mathcal{O}(N^3 \log_2 N)$ by applying a hierarchical, recursive decomposition to the backprojection operation [8], which the could yield an $\mathcal{O}(N^3 \log_2 N)$ reconstruction algorithm for cone-beam tomography, if combined with a fast 2D reprojection algorithm to compute the 2D Radon transforms from cone-beam to 3-D Radon data [11]. These techniques are yet to be applied to laminographic reconstruction.

3.3 Iterative Reconstruction Techniques

In contrast to FBP algorithms, iterative reconstruction techniques do not require modification to be applicable to laminar reconstruction, whether the scan

trajectory leads to varying or constant magnification. In theory, all that is required is the specification of the appropriate system matrix that describes the laminar measurement geometry, and indeed these algorithms have been applied to laminographic reconstructions since the late 1980s [7]. Many iterative methods are broadly classed as algebraic techniques, although an iterative version of the classically non-iterative filtered backprojection algorithm has also been developed to reconstruct laminographic differential phase measurements [37].

As CL system geometries do not generally provide as much spatial information as CT geometries, the system matrix tends to be ill-conditioned or non-invertible. Additional regularisation is thus often applied when using iterative techniques for CL applications. Furthermore, these methods come with an additional computational cost compared to the FBP methods. One possible approach to overcome these limitations is the use of advanced computational hardware as discussed in § 3.5.

3.3.1 ART

The algebraic reconstruction technique (ART) (known in applied mathematics as the Kaczmarz algorithm [47]) has been introduced into the CT community in the 1970s, when it was proposed independently by Hounsfield [3, 42], and by Gordon, Bender and Herman [32]. In ART, the object volume is represented as a matrix of voxels. A system of linear equations is set up to find the attenuations due to each voxel in the sample: the total attenuation for each ray is known from the projections. Each ray path through the object is represented as an equation and these are combined into a matrix, whose inversion gives the

solution. The runtime of a true matrix inversion with $\mathcal{O}(10^9)$ unknowns would be prohibitively long, so an iterative approximation method is typically used instead, where the attenuation calculated from each ray path through the current trial voxel array is compared to the recorded attenuation. The differences are used to inform improvements to the trial solution by adjusting the attenuation values of pixels along the given ray path, until some stopping criteria is met.

These techniques typically take considerably longer to run than tomosynthesis or backprojection methods, but can yield an improved reconstruction quality. Commercially implemented algebraic reconstruction algorithms are often GPU-accelerated and using a high-end, multi-GPU workstation, a volume of $\mathcal{O}(10^9)$ voxels may be iteratively reconstructed relatively rapidly.

Recent work has shown that a multi-resolution approach may be adopted for algebraic CT reconstruction methods, and this reduces both the computational burden and the amount of memory required. It is claimed that these reductions in required resources can be achieved without significantly affecting the quality of the reconstructed image [21].

The ART can easily be modified to integrate *a priori* knowledge about the system and/or the imaged object (e.g. a known shape of the sample or constraints on the values of the reconstructed function) into the algorithm, which may improve the fidelity of the reconstruction whilst decreasing the computational requirements [61]. The ART has long been considered to provide better results where only limited numbers of projections or projections from limited angular ranges are available [4, 85], or where *a priori* information can be included, the latter potentially giving reduced reconstruction times and suppres-

sion of artefacts [31].

3.3.2 SIRT

The simultaneous iterative reconstruction technique (SIRT) was introduced in 1972 [30] as an alternative to the previously introduced ART. It was shown to produce correct reconstructions under certain conditions, as compared to the ART which does not produce exact reconstructions in general. More recent general advancements of the technique include the tuning of the relaxation parameter that is frequently used to accelerate the method, and the introduction of a scalar preconditioning scheme [35]. Moreover, a modified form of the SIRT has been proposed for laminographic application, known as the discrete algebraic reconstruction technique (DART) [9]. This method assumes that the object being reconstructed consists only of a very limited number of materials (e.g. 2–5), which correspond to characteristic grey levels in the reconstruction; promising results were achieved using a simulated reconstruction of a phantom representing a slab of silicon containing a grid of copper through-silicon vias, as might typify an electronic component, some of which contain voids. This technique is, however, only suited to objects that may be well represented using a small number of grey levels – a class of objects that includes many real-world engineering components, which are frequently composites of only few phases.

3.3.3 Simultaneous algebraic reconstruction technique: SART

The simultaneous algebraic reconstruction technique (SART) was proposed in 1984 as a superior implementation of the original Algebraic Reconstruction

Technique, making a good reconstruction achievable with only one iteration. In the SART, error-correction terms are computed as they are in ART, but applied simultaneously for all rays in a given projection. The method was developed with the goal of decreasing the appearance of the so-called salt and pepper noise artefacts in images reconstructed via ART [5]. The Andersen implementation of SART reduces the number of equations used per projection c.f. the numbers used in ART; in the former, the number of equations used is approximately the number of points in the reconstructed image whereas in the latter, the system was typically overdetermined by a factor of around four. Recent work that applied a GPU-accelerated SART algorithm to reconstruct a laminographic reconstruction of some $2000 \times 2000 \times 300$ voxels reported a run time just in excess of an hour for a single iteration [56].

A significant improvement in image quality in laminographic SART may be achieved by compensating for artefacts arising from the fact that laminographic projections are often truncated (i.e. do not always show the whole of the object in question). The truncation errors typically consist of increased absorption values near the edges of the volume reconstructed, and with an iterative reconstruction, this can lead to reduced absorption values in the interior and decreased contrast. Recent work applied a ray-length based region of interest correction technique and yielded very much improved contrast over the uncorrected results in real scans [71].

3.3.4 Maximum likelihood and statistical reconstruction

A method was proposed in 1982 which applied maximum likelihood methods to the problem of emission tomography reconstruction [73]. The simula-

tions carried out by Shepp and Vardi indicated that this method could provide a lower statistical noise artefact over convolution backprojection methods, but without introducing excessive smoothing. Maximum likelihood techniques have also been applied to artefact suppression in cone-beam CT, "nearly eliminating" the truncation artefacts in two out of three scans of humans in one study, and qualitatively improving the images in all cases [58]. More recently, ordered subsets expectation maximisation methods have been applied to emission tomography, delivering an order-of-magnitude acceleration over a standard expectation maximisation algorithm in simulated emission tomography [44]. In these methods, projection data are grouped into an ordered sequence of blocks, and an iteration consists of a pass through all the blocks – in each block, the current estimate is used to initialise an application of standard EM. A maximum likelihood method was developed for tomosynthesis mammography, illustrating the method's applicability to laminographic scanning [81].

3.4 Regularisation and prior information

As CL does not provide the same level of 3D information that is usually available in CT, reconstruction greatly benefits from the use of prior information and regularisation. For example, in scanning biological specimens, the knowledge that vascular anatomy consists of a void in which a "dilute framework" of nonzero density values is embedded motivated the development of an iterative reconstruction method for digital tomosynthesis that gave rise to a clear improvement in image quality as early as 1988 [51]. Iterative methods have the advantage that it is often relatively easy to incorporate such additional con-

straints.

Statistical methods incorporating *a priori* information, such as the previously-known shape of the object to be reconstructed, or which use prior information about the type of reconstructed image that is required as one of an ensemble (e.g. in a medical context, an ensemble might contain many images of various hearts; this provides prior information that may be applied to reduce artefacts in reconstructing a scanned heart), are classed as Bayesian methods. Bayesian methods are appealing for applications such as laminography where limited data is available, because they permit the inclusion through the ensemble of information beyond that which may be obtained through laminographic imaging alone, and which may help to reduce artefacts. Early Bayesian methods are reviewed in [36], which considers techniques such as maximum a posteriori (MAP) and fit and iterative reconstruction (FAIR). Bayesian methods for emission tomographic reconstruction were developed by Hebert and Leahy [38], and Green [34]. More recent work has demonstrated the applicability of an iterative expectation maximisation algorithm to laminographic reconstructions [50].

Although in many cases the image to be reconstructed is not sparse, the image formed from the magnitude of its gradient is often approximately sparse. This motivates the development of iterative methods for divergent-beam reconstructions based on total variation (TV) minimisation [74, 75]. The reconstruction is posed as an optimisation problem where the TV of the reconstructed image is minimised. This has been shown to perform well in cases where there are few projections, projections for a limited angular range only, or projections containing gaps due to bad detector bins, making these methods naturally

suited to laminographic reconstruction. Under certain conditions the optimisation can yield a unique solution, which is the true image [14, 15].

More recent work [29] introduces a hybrid reconstruction technique that utilises an initial reconstruction from an FBP or linogram technique [23], followed by a Gerchberg-Papoulis extrapolation [17] using the linogram (GPEL) which compensates for missing data, applied in an iterative-reconstruction-reprojection algorithm [62]. Because the GPEL method may be divergent when the data are noisy or undersampled, TV minimisation is embedded into the GPEL algorithm, in a process called GPEL-TV. Preliminary results indicate that the algorithm can reconstruct high-quality images from noisy and undersampled data in security inspection systems. TV regularisation is one common approach taken in several recent advances in compressed sensing based reconstruction techniques, which are a class of techniques aiming to exploit sparsity of the image data to recover it from fewer projections than conventional methods would require. Some of these techniques have been applied with good results to laminographic reconstruction problems: just 40 projections were required to produce good reconstructions of a resolution test phantom in one computational simulation (where a novel system trajectory was also employed, as discussed in § 2.4) [1]. Another compressed sensing based tomosynthesis reconstruction technique was recently developed by Ertas et al. [24], employing a combination of local TV minimisation and non-local means filtering. This method yields results visually superior to widely used algebraic reconstruction methods using TV alone, exhibiting reduced noise whilst preserving edge definition.

Another recent approach for reducing artefacts is based on making a pre-

scan with the goal of detecting the outer surfaces of the specimen, perhaps using contrasting markers. The knowledge about the specimen that this pre-scan provides can then be used to regularise a tomosynthesis reconstruction, or serve as prior information for an iterative reconstruction method [78].

3.5 GPU- and parallel computing accelerated techniques

Reconstruction has always been a compute-intensive process, whichever method is employed. Initial efforts at accelerating the process focused on expensive hardware costing tens of thousands of dollars. However, as long ago as 2005, consumer graphics processing units (GPUs) were a promising choice for accelerating various techniques using in CT reconstruction: one paper that year applied the GPU to FDK, SART and EM reconstructions [83]. At that time, general-purpose GPU programming was considerably less well-developed than it is today. Languages for heterogeneous computing such as OpenCL [49, 77] were not available, and GPU memory was more limited (256 MiB being typical, facilitating reconstructed volumes of 128^3 voxels; 4 GiB is easily and economically available on a consumer-grade GPU today, and cards featuring 16 GiB are available at the time of writing).

Recent work by Scherl et al investigates various computational platforms for FDK CT reconstruction, finding speedups of 6.5 for the Cell Broadband Engine Architecture (using 2 processors), 22.0 for a single GPU board, and 35.8 for nine FPGA chips, where the reference time was that taken by a quad-core workstation with no ancillary processor [70]. However, Scherl et al do caution that efficiently utilising such parallel computational hardware brings the disadvantage of requiring considerably more complicated implementations. The

speedup for a single GPU achieved by Scherl et al of 22× is in broad agreement with the speedup of 24×, achieved for the FDK algorithm in 2010 by other researchers [64]. More dramatic speedups to the FDK method (from 25 minutes on the CPU to 3.2 seconds on a GPU) were reported by yet other workers [63]. However, it is difficult and perhaps subjective to ensure that, when an algorithm is implemented on multiple architectures, it is equally well-optimised to get the best results from the strengths of each of them, so the reported speedups should be considered indicative only. The SART reconstruction algorithm has also been shown to be amenable to acceleration by running on GPUs, with one group reporting a speedup of greater than 64 times, compared to a "state-of-the-art CPU" [48]. More recently, another group has implemented the SART algorithm for laminographic reconstruction on a GPU and achieved speedups between 8× and 55× compared to their single-core CPU implementation [56].

4 Summary and outlook

Whilst CT is now an established technique in medical, materials engineering, industrial manufacturing and nondestructive testing applications, computed laminography – especially in cone beam systems – is still undergoing considerable development. When scanning objects whose aspect ratios complicate or preclude the use of a full CT scan, CL is becoming a compelling alternative.

We have examined recent advances in computed laminography, both in terms of surveying scanner geometries and trajectories, and reconstruction approaches that have been adapted for laminography. We first considered and illustrated scan geometries including linear and circular planar, swing (also

known as limited-angle CT), rotary, and one example of a more complex, non-traditional scan trajectory that yielded promising results in initial simulation studies. We then considered various reconstruction methods that have been applied to laminography, starting with the most basic digital tomosynthesis, and then considering filtered backprojection – a technique that is popular and well-developed in CT, and has been applied to some laminographic systems with success. The iterative reconstruction methods have long been applied to laminographic reconstruction and we considered them next, before turning our attention to the various regularisation techniques, and *a priori* information, that can be applied to enhance these reconstructions. We finally considered the application of graphical processing units and other parallel computing acceleration techniques, which can offer significant speedups of several tens of times compared to conventional methods. This could make reconstruction methods that previously would have had prohibitively high runtimes increasingly practical in real applications.

Analogously to CT, CL may be performed using either cone or parallel-beam geometries; we have mostly considered cone-beam systems in the present work, due to their advantages which include the availability of lab-based sources and the magnification that is achievable using the cone beam. However, laminography is a less well established technique, and therefore is undergoing more rapid development. We have seen that many developments first made in CT are now being applied to CL and this is a trend that is likely to continue, due to the similarity of the two techniques. As time goes on, both interest in computed laminography and the capability of computational resources to facilitate rapid simulation and reconstruction are increasing, so that the pace of development

remains high.

Acknowledgement

The authors gratefully acknowledge funding from Innovate UK, the UK's innovation agency through ProjectCAN, TSB grant 101804. The ProjectCAN consortium includes QinetiQ, University College London, University of Southampton, Nikon, Axi-Tek and Rolls Royce.

References

[1] S. Abbas, M. Park, J. Min, H. K. Kim, and S. Cho. Sparse-view computed laminography with a spherical sinusoidal scan for nondestructive testing. *Opt. Express*, 22(15):17745–17755, Jul 2014.

[2] V. Altapova, L. Helfen, A. Myagotin, D. Hänschke, J. Moosmann, J. Gunneweg, and T. Baumbach. Phase contrast laminography based on talbot interferometry. *Opt. Express*, 20(6):6496–6508, Mar 2012.

[3] J. Ambrose and G. Hounsfield. Computerized transverse axial tomography. *British J. Radiology*, 46:148–149, 1973.

[4] A. Andersen. Algebraic reconstruction in CT from limited views. *Medical Imaging, IEEE Trans. on*, 8(1):50–55, Mar 1989.

[5] A. Andersen and A. Kak. Simultaneous Algebraic Reconstruction Technique (SART): A superior implementation of the ART algorithm. *Ultrasonic Imaging*, 6(1):81 – 94, 1984.

[6] C. Axelsson and P. Danielsson. Three-dimensional reconstruction from cone-beam data in $\mathcal{O}(N^3 \log N)$ time. *Physics in Medicine and Biology*, 39(3):477, 1994.

[7] M. D. Barker. Laminographic reocnstruction from real-time radiogrpahic images. In D. O. Thompson and D. E. Chimenti, editors, *Review of progress in quantitative NDE*, volume 8a, pages 457–464. Plenum Press, New York, 1989.

[8] S. Basu and Y. Bresler. $\mathcal{O}(N^3 \log_2 N)$ filtered backprojection reconstruction algorithm for tomography. *Medical Image Process., IEEE Trans. on*, 21(2):76–88, February 2002.

[9] K. J. Batenburg, W. J. Palenstijn, and J. Sijbers. 3D imaging of semiconductor components by discrete laminography. *AIP Conf. Proc.*, 1601:168–179, 2014.

[10] E. C. Beckmann. CT scanning: the early days. *British J. Radiology*, 79:5–8, 2006.

[11] A. Boag, Y. Bresler, and E. Michielssen. A multilevel domain decomposition algorithm for fast $\mathcal{O}(N^2 \log N)$ reprojection of tomographic images. *Image Process., IEEE Trans. on*, 9(9):1573–1582, Sep 2000.

[12] D. Boyd, W. Herrmannsfeldt, J. Quinn, and R. Sparks. X-ray transmission scanning system and method and electron beam x-ray scan tube for use therewith, Sept. 28 1982. US Patent 4352021.

[13] D. Bull, L. Helfen, I. Sinclair, S. Spearing, and T. Baumbach. A comparison of multi-scale 3D X-ray tomographic inspection techniques for assessing

carbon fibre composite impact damage. *Composites Sci. and Technology*, 75:55–61, February 2013.

[14] E. Candès, J. Romberg, and T. Tao. Robust uncertainty principles: exact signal reconstruction from highly incomplete frequency information. *Inform. Theory, IEEE Trans. on*, 52(2):489–509, Feb 2006.

[15] E. Candes and T. Tao. Near-optimal signal recovery from random projections: Universal encoding strategies? *Inform. Theory, IEEE Trans. on*, 52(12):5406–5425, Dec 2006.

[16] G. Cao, Y. Z. Lee, R. Peng, Z. Liu, R. Rajaram, X. Calderon-Colon, L. An, P. Wang, T. Phan, S. Sultana, D. S. Lalush, J. P. Lu, and O. Zhou. A dynamic micro-CT scanner based on a carbon nanotube field emission x-ray source. *Physics in Medicine and Biology*, 54(8):2323, 2009.

[17] P. Chatterjee, S. Mukherjee, S. Chaudhuri, and G. Seetharaman. Application of Papoulis-Gerchberg method in image super-resolution and inpainting. *Comput. J.*, 52(1):80–89, Jan. 2009.

[18] M. K. Cho, H. Youn, S. Y. Jang, and H. K. Kim. Cone-beam digital tomosynthesis for thin slab objects. *NDT & E Int.*, 47:171 – 176, 2012.

[19] V. Cnudde, B. Masschaele, M. Dierick, J. Vlassenbroeck, L. V. Hoorebeke, and P. Jacobs. Recent progress in x-ray CT as a geosciences tool. *Appl. Geochemistry*, 21(5):826 – 832, 2006. Frontiers in Analytical Geochemistry—An IGC 2004 Perspective.

[20] D. J. De Rosier and A. Klug. Reconstruction of three dimensional structures from electron micrographs. *Nature*, 217:130–134, January 1968.

[21] Y. De Witte, J. Vlassenbroeck, and L. Van Hoorebeke. A multiresolution approach to iterative reconstruction algorithms in x-ray computed tomography. *Image Process., IEEE Trans. on*, 19(9):2419–2427, Sept 2010.

[22] A. Delaney and Y. Bresler. Globally convergent edge-preserving regularized reconstruction: an application to limited-angle tomography. *Image Process., IEEE Trans. on*, 7(2):204–221, Feb 1998.

[23] P. Edholm and G. Herman. Linograms in image reconstruction from projections. *Medical Imaging, IEEE Trans. on*, 6(4):301–307, Dec 1987.

[24] M. Ertas, I. Yildirim, M. Kamasak, and A. Akan. An iterative tomosynthesis reconstruction using total variation combined with non-local means filtering. *BioMedical Eng. OnLine*, 13, 2014.

[25] L. A. Feldkamp, L. C. Davis, and J. W. Kress. Practical cone-beam algorithm. *J. Opt. Soc. Am. A*, 1(6):612–619, Jun 1984.

[26] J. Fu, T. Biernath, M. Willner, M. Amberger, J. Meiser, D. Kunka, J. Mohr, J. Herzen, M. Bech, and F. Pfeiffer. Cone-beam differential phase-contrast laminography with x-ray tube source. *EPL (Europhysics Lett.)*, 106(6):68002, 2014.

[27] J. Fu, B. Jiang, and B. Li. Large field of view computed laminography with the asymmetric rotational scanning geometry. *Sci. China Technological Sci.*, 53(8):2261–2271, 2010.

[28] H. Gao, L. Zhang, Z. Chen, Y. Xing, J. Cheng, and Z. Qi. Direct filtered-backprojection-type reconstruction from a straight-line trajectory. *Optical Engineering*, 46(5):057003–057003–11, 2007.

[29] H. Gao, L. Zhang, Z. Chen, Y. Xing, H. Xue, and J. Cheng. Straight-line-trajectory-based x-ray tomographic imaging for security inspections: system design, image reconstruction and preliminary results. *Nucl. Sci., IEEE Trans. on*, 60(5):3955–3968, Oct 2013.

[30] P. Gilbert. Iterative methods for the reconstruction of three dimensional objects from their projections. *J. Theoretical Biology*, 36:105–117, 1972.

[31] S. Gondrom, J. Zhou, M. Maisl, H. Reiter, M. Kröning, and W. Arnold. X-ray computed laminography: an approach of computed tomography for applications with limited access. *Nucl. Eng. and Design*, 190(1-2):141–147, 1999.

[32] R. Gordon, R. Bender, and G. T. Herman. Algebraic Reconstruction Techniques (ART) for three-dimensional electron microscopy and X-ray photography. *J. Theoretical Biology*, 29(3):471 – 481, 1970.

[33] P. P. Grangeat, P. Le Masson, P. Melennec, and P. Sire. Evaluation of the 3-D Radon transform algorithm for cone beam reconstruction. In M. H. Loew, editor, *Medical Imaging V: Image Process.*, volume 1445 of *Soc. of Photo-Optical Instrumentation Eng. (SPIE) Conf. Series*, pages 320–331, June 1991.

[34] P. Green. Bayesian reconstructions from emission tomography data using a modified EM algorithm. *Medical Imaging, IEEE Trans. on*, 9(1):84–93, Mar 1990.

[35] J. Gregor and T. Benson. Computational Analysis and Improvement of SIRT. *Medical Imaging, IEEE Trans. on*, 27(7):918–924, July 2008.

[36] K. M. Hanson. Bayesian and related methods in image reconstruction from incomplete data. In *Image Recovery: Theory and Applicat.* Academic Press, 1987.

[37] S. Harasse, W. Yashiro, and A. Momose. Iterative reconstruction in x-ray computed laminography from differential phase measurements. *Opt. Express*, 19(17):16560–16573, Aug 2011.

[38] T. Hebert and R. Leahy. A generalized EM algorithm for 3-D Bayesian reconstruction from Poisson data using Gibbs priors. *Medical Imaging, IEEE Trans. on*, 8(2):194–202, Jun 1989.

[39] L. Helfen, T. Baumbach, P. Pernot, P. Mikulk, M. DiMichiel, and J. Baruchel. High-resolution three-dimensional imaging by synchrotron-radiation computed laminography. *Proc. SPIE*, 6318:63180N–63180N–9, 2006.

[40] L. Helfen, A. Myagotin, P. Mikulík, P. Pernot, A. Voropaev, M. Elyyan, M. Di Michiel, J. Baruchel, and T. Baumbach. On the implementation of computed laminography using synchrotron radiation. *Review of Scientific Instruments*, 82(6), 2011.

[41] L. Helfen, F. Xu, H. Suhonen, P. Cloetens, and T. Baumbach. Laminographic imaging using synchrotron radiation – challenges and opportunities. *J. Physics: Conf. Series*, 425(19):192025, 2013.

[42] G. Hounsfield. Computerized transverse axial scanning (tomography). Part 1. Description of system. *British J. Radiology*, 46:1016–1022, 1973.

[43] J. Hsieh, B. Nett, Z. Yu, K. Sauer, J.-B. Thibault, and C. A. Bouman. Recent Advances in CT Image Reconstruction. *Current Radiology Reports*, 1(1):39–51, 2013.

[44] H. Hudson and R. Larkin. Accelerated image reconstruction using ordered subsets of projection data. *IEEE Trans Med Imaging.*, 13(4):601–609, January 1994.

[45] JAMA. Editorial: Andre Bocagé (1892-1953) – French tomographer. *J. of the Amer. Medical Assoc.*, 193(3):233, 1965.

[46] Q. Jie-Min, C. Da-Quan, Z. Wei, T. Xiao, S. Cui-Li, W. Yan-Fang, W. Cun-Feng, S. Rong-Jian, W. Long, Y. Zhong-Qiang, and Y. Yong-Lian. Computed laminography and reconstruction algorithm. *Chinese Physics C*, 36(8):777, 2012.

[47] S. Kaczmarz. Angenäerte auflöung von systemen linearer gleichungen. *Bulletin Int. de l'Académie Polonaise des Sci. et des Lettres. Classe des Sci. Mathématiques et Naturelles. Série A, Sci. Mathématiques*, 35:355–357, 1937.

[48] B. Keck, H. Hofmann, H. Scherl, M. Kowarschik, and J. Hornegger. GPU-accelerated SART reconstruction using the CUDA programming environment. In *Proc. SPIE*, volume 7258, pages 72582B–72582B–9, 2009.

[49] Khronos OpenCL Working Group. The OpenCL Specification version 1.0. manual, Khronos Group, 2009.

[50] M. Kroupa and J. Jakubek. High contrast laminography using iterative algorithms. *J. Instrumentation*, 6(01):C01045, 2011.

[51] R. A. Kruger. Reconstruction of blood vessels from x-ray substraction projections. In *Eng. in Medicine and Biology Soc., 1988. Proc. of the Annu. Int. Conf. of the IEEE*, pages 401–403 vol.1, Nov 1988.

[52] H. Kudo and T. Saito. Derivation and implementation of a cone-beam reconstruction algorithm for nonplanar orbits. *Medical Imaging, IEEE Trans. on*, 13(1):196–211, Mar 1994.

[53] M. Kurfiss and G. Streckenbach. Digital Laminography and Computed Tomography with 600 kV for Aerospace Applications. In *Proc.* 4^{th} *Int. Symp. on NDT in Aerospace.*, 2012.

[54] G. Lauritsch and W. H. Haerer. Theoretical framework for filtered back projection in tomosynthesis. *Proc. SPIE*, 3338:1127–1137, 1998.

[55] T. Liu. Cone-beam CT reconstruction for planar object. *NDT & E Int.*, 45(1):9 – 15, 2012.

[56] M. Maisl, L. Marsalek, C. Schorr, J. Horacek, and P. Slusallek. GPU-accelerated Computed Laminography with Application to non-destructive Testing. In *Proc.* 11^{th} *European Conf. on Non-Destructive Testing (ECNDT 2014)*, 2014.

[57] M. Maisl, F. Porsch, and C. Schorr. Computed laminography for x-ray inspection of lightweight constructions. In *Proc.* 2^{nd} *Int. Symp. on NDT in Aerospace.*, 2010.

[58] S. H. Manglos. Truncation artifact suppression in cone-beam radionuclide transmission CT using maximum likelihood techniques: evaluation with human subjects. *Phys. Med. Biol.*, 37(3):549–562, 1992.

[59] K. R. Maravilla, R. C. Murry, and S. Horner. Digital tomosynthesis: technique for electronic reconstructive tomography. *Amer. J. Neuroradiology*, 4(4):883–8, 1983.

[60] H. Matsuo, A. Iwata, I. Horiba, and N. Suzumura. Three-dimensional image reconstruction by digital tomo-synthesis using inverse filtering. *Medical Imaging, IEEE Trans. on*, 12(2):307–313, Jun 1993.

[61] A. Myagotin, A. Voropaev, L. Helfen, D. Hänschke, and T. Baumbach. Efficient volume reconstruction for parallel-beam computed laminography by filtered backprojection on multi-core clusters. *Image Process., IEEE Trans. on*, 22(12):5348–5361, Dec 2013.

[62] M. Nassi, W. R. Brody, B. P. Medoff, and A. Macovski. Iterative reconstruction-reprojection: an algorithm for limited data cardiac-computed tomography. *Biomedical Eng., IEEE Trans. on*, BME-29(5):333–341, May 1982.

[63] P. B. Noël, A. M. Walczak, J. Xu, J. J. Corso, K. R. Hoffmann, and S. Schafer. GPU-based cone beam computed tomography. *Comput. Methods and Programs in Biomedicine*, 98(3):271–277, 2010. HP-MICCAI 2008.

[64] Y. Okitsu, F. Ino, and K. Hagihara. High-performance cone beam reconstruction using CUDA compatible GPUs. *Parallel Computing*, 36(2-3):129–141, 2010.

[65] PerkinElmer Inc, Santa Clara, CA. Product Note: XRD 1611 xP Flat Panel X-ray Detector. `http://www.perkinelmer.co.uk/PDFs/downloads/011104A_01-PRD.pdf`, Accessed 2015.

[66] M. Rehak, U. Hassler, and R. Hanke. Acquisition trajectories for x-ray tomosynthesis applied to planar samples. In *Proc.* 2nd *Int. Symp. on NDT in Aerospace*, 2010.

[67] S. Rooks and T. Sack. X-ray inspection of flip chip attach using digital tomosynthesis. *Circuit World*, 21(3):51–55, 1995.

[68] J. E. Rouse. *Characterisation of Impact Damage in Carbon Fibre Reinforced Plastics by 3D X-Ray Tomography*. PhD thesis, The University of Manchester, Manchester, UK, 10 2012.

[69] B. D. Sawicka. Computed laminography, limited-view tomography and fully 3-D image reconstruction. In M. C. et al, editor, *Proc. 1995 Symp. on Appl. Math.*, Deep River, Canada, 1995. Atomic Energy of Canada Ltd Report RC-1458, CMS-95-03, pp. 70-73.

[70] H. Scherl, M. Kowarschik, H. G. Hofmann, B. Keck, and J. Hornegger. Evaluation of state-of-the-art hardware architectures for fast cone-beam CT reconstruction. *Parallel Computing*, 38(3):111 – 124, 2012.

[71] C. Schorr and M. Maisl. A ray-length-based ROI-correction for computed laminography. In *Conf. Ind. Computed Tomography, ICT 2014*, pages 253–258, 2014.

[72] M.-M. Seger, N. Karlstroms, and P. Edholm. The relation between 3D linear CT and linear filtered tomosynthesis. Application to crack estimation in tubes. In *Proc. 1999 Int. Meeting on Fully Three-Dimensional Image Reconstruction in Radiology and Nucl. Medicine*, pages 163–166, 1999.

[73] L. Shepp and Y. Vardi. Maximum likelihood reconstruction for emission tomography. *Medical Imaging, IEEE Trans. on*, 1(2):113–122, Oct 1982.

[74] E. Y. Sidky, C.-M. Kao, and X. Pan. Accurate image reconstruction from few-views and limited-angle data in divergent-beam CT. *ArXiv e-prints*, Apr 2009.

[75] E. Y. Sidky and X. Pan. Image reconstruction in circular cone-beam computed tomography by constrained, total-variation minimization. *Physics in Medicine and Biology*, 53(17):4777, 2008.

[76] B. Smith. Image reconstruction from cone-beam projections: Necessary and sufficient conditions and reconstruction methods. *Medical Imaging, IEEE Trans. on*, 4(1):14–25, March 1985.

[77] J. E. Stone, D. Gohara, and G. Shi. OpenCL: A Parallel Programming Standard for Heterogeneous Computing Systems. *IEEE Des. Test*, 12(3):66–73, May 2010.

[78] K. Tigkos, U. Hassler, W. Holub, N. Woerlein, and M. Rehak. Regularization approach for tomosynthesis x-ray inspection. *AIP Conf. Proc.*, 1581(1):1793–1799, 2014.

[79] H. Tuy. An inversion formula for cone-beam reconstruction. *SIAM J. Appl. Math.*, 43(3):546–552, 1983.

[80] Y. Wang, Z. Ou, and F. Wang. Modified FDK algorithm for cone-beam reconstruction with efficient weighting scheme. In *Intelligent Control and Automation, 2006. WCICA 2006. The Sixth World Congress on*, volume 2, pages 9703–9707, 2006.

[81] T. Wu, J. Zhang, R. Moore, E. Rafferty, D. Kopans, W. Meleis, and D. Kaeli. Digital tomosynthesis mammography using a parallel maximum-likelihood reconstruction method. *Proc. SPIE*, 5368:1–11, 2004.

[82] F. Xu, L. Helfen, T. Baumbach, and H. Suhonen. Comparison of image quality in computed laminography and tomography. *Opt. Express*, 20(2):794–806, Jan 2012.

[83] F. Xu and K. Mueller. Accelerating popular tomographic reconstruction algorithms on commodity pc graphics hardware. *Nucl. Sci., IEEE Trans. on*, 52(3):654–663, June 2005.

[84] M. Yang, G. Wang, and Y. Liu. New reconstruction method for x-ray testing of multilayer printed circuit board. *Optical Eng.*, 49(5):056501–056501–6, 2010.

[85] J. Zhou, M. Maisl, H. Reiter, and W. Arnold. Computed laminography for materials testing. *Appl. Physics Lett.*, 68(24):3500–3502, 1996.

Figure captions

Fig. 1 Schematic representation of the linear laminographic system motion, which involves linear translation of the specimen relative to source and detector.

Fig. 2 A schematic representation of the circular laminographic system motion, which involves rotating the source and detector around a common centre.

Fig. 3 A schematic representation of swing laminography, which is also known as limited-angle CT and involves an incomplete rotation of the specimen about an axis 90° to the principle ray.

Fig. 4 A schematic representation of rotary laminography, which is analogous to CT, but has the axis of rotation inclined to the beam's principal ray.

Fig. 5 Schematic illustration of the spherical sinusoidal scanning trajectory, a relatively complicated motion proposed by [1].

Figures

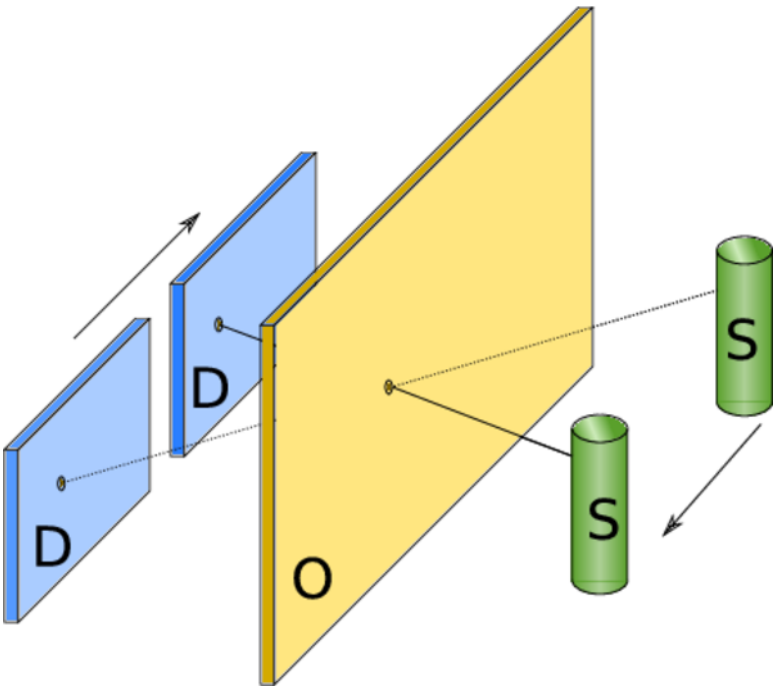

Fig. 1

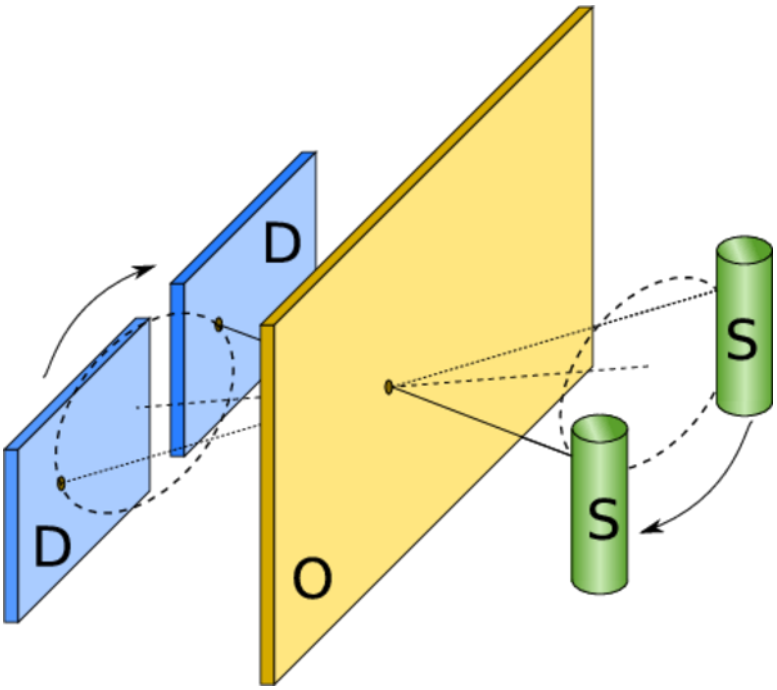

Fig. 2

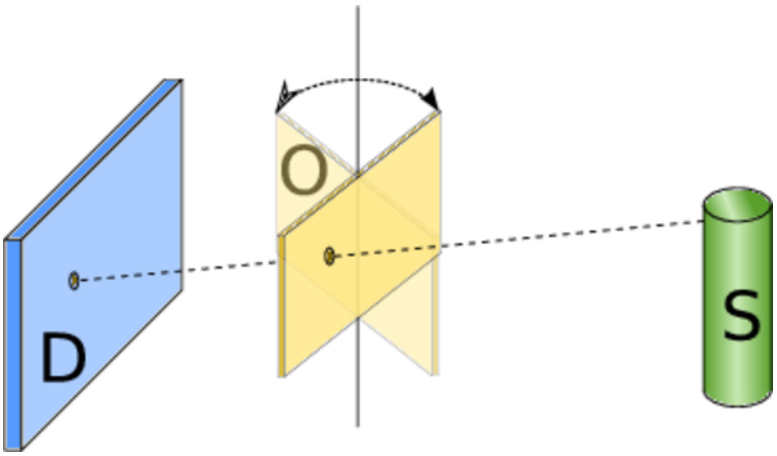

Fig. 3

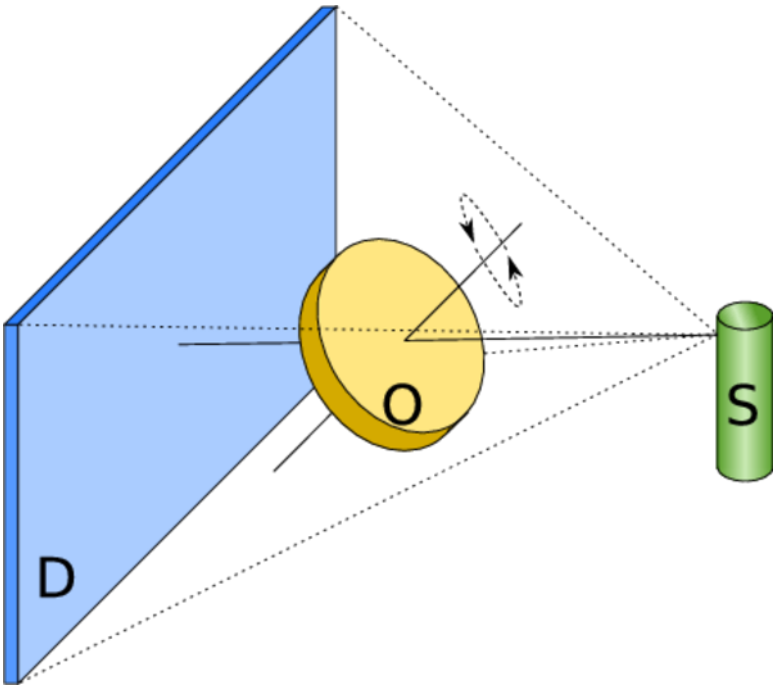

Fig. 4

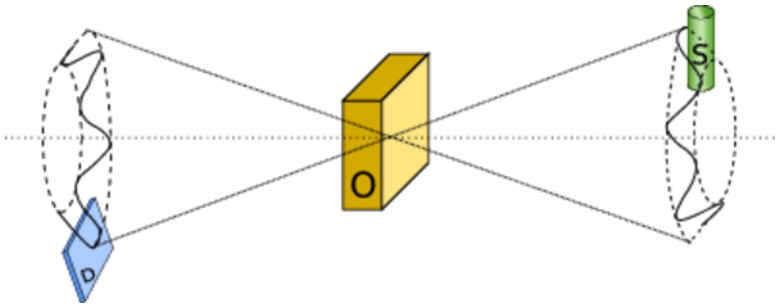

Fig. 5